Hydraulic bore interaction with a column - A comparison between the solution of the shallow equation and experimental results

Xinsheng Qin xsqin@uw.edu
Kaspar Mueller kasparm@uw.edu

March 11, 2015

Abstract

In this paper we compare the solution of the shallow water equations with experimental results. The experiment simulates the interaction between an incident bore and a free-standing coastal structure. The shallow water equations are solved using the GeoClaw solver of the CLAWPACK software.

Three different cases are simulated and compared. In the first case a simple dam break problem is performed and evaluated. The history of the wave height and velocity at the center location, where the column will be mounted are compared. In the second case, a square column is added and wave height at various locations in front of the column are measured and compared. For the third case, the square column is replaced by a cylinder column and the same variables are measured and compared. The discrepancy between the GeoClaw simulation and the experimental results are discussed and analyzed.

1 Introduction

The aim of this work is to compare computational results using CLAWPACK with experimental results. This is done for the interaction of a bore and a free-standing coastal structure. The experiment results are given by Halldór Árnason [1]. We model the water using the shallow water equations which will be introduced in Section 2. We solve these equations using CLAWPACK's GeoClaw solver which is specialized for geophysical flow problems. In Section 3 we show how GeoClaw solves the shallow water equations and how it handles the topography. In Section 4 we describe the setup of the test case. We focus on three cases. First we compare wave height and velocity for the pure dambreak without structure in the domain in Section 5. Second we add a square column and compare wave height upstream as well as downstream of the column in 6. Lastly in Section 7 we compare the wave height at the same location but for a cylinder column. We close this paper with a conclusion in Section 8.

2 The shallow water equations

We write the 2D depth averaged shallow water equations as

$$h_t + (uh)_x + (vh)_y = 0 \tag{1}$$

$$(hu)_t + (huv)_y + (hu^2 + \frac{1}{2}gh^2)_x = -ghB_x - Du \tag{2}$$

$$(hv)_t + (huv)_x + (hv^2 + \frac{1}{2}gh^2)_y = -ghB_y - Dv \tag{3}$$

where u, v are the horizontal depth averaged velocities, B the topography and D the drag coefficient. g denotes the gravitational acceleration. In the present case the topography will be flat except the column located downstream. The drag coefficient D is given by

$$D = \frac{gM^2\sqrt{(u^2 + v^2)}}{h^{5/3}} \tag{4}$$

where M is the Manning coefficient which is $M = 0.015$. The Manning coefficient is an empirical coefficient that includes the roughness of the surface. The initial condition is given by a jump in the water depth h. The water is initially at rest.

3 The Algorithm in CLAWPACK/GeoClaw

We solve the shallow water equations with CLAWPACK. Specifically we used the GeoClaw solver which used a special version of the f-wave approach described in [2]. This solver combines the qualities of the Roe solver, HLLE-type solver and the f-wave approach. From the Roe solver it has the quality of giving a exact solution for a single-shock Riemann problem. Like the HLLE solver this method is depth positive semidefinite. The method has also a natural entropy-fix and gives a better approximation for problems with large rarefactions. The solver also maintains large class of steady states. The topography and drag term are incorporated in the Riemann problem. Stability and accuracy are improved by solving a transverse Riemann problem, where the waves moving normal to the cell are split into traverse direction.

$$
\begin{aligned}
Q_{ij}^{n+1} &= Q_{ij}^n - \frac{\Delta t}{\Delta x}\left(\mathcal{A}^+\Delta Q_{i-1/2,j}^n + \mathcal{A}^-\Delta Q_{i+1/2,j}^n\right) - \frac{\Delta t}{\Delta y}\left(\mathcal{B}^+\Delta Q_{i,j-1/2}^n + \mathcal{B}^-\Delta Q_{i,j+1/2}^n\right) \\
&\quad - \frac{\Delta t}{\Delta x}\left(\tilde{F}_{i+1/2,j}^n - \tilde{F}_{i-1/2,j}^n\right) - \frac{\Delta t}{\Delta y}\left(\tilde{G}_{i,j+1/2}^n - \tilde{G}_{i,j-1/2}^n\right)
\end{aligned} \tag{5}
$$

In the f-wave approache the flux is decomposed the following way

$$f(Q_i) - f(Q_{i-1}) = \sum_{p=1}^m \mathcal{Z}_{i-1/2}^p = \sum_{p=1}^m \beta_{i-1/2}^p r_{i-1/2}^p \tag{6}$$

where we write this in one dimensional form since one dimensional Riemann solvers are used. Instead of waves $\mathcal{W}$ representing the jump in Q we have now waves $\mathcal{Z}$ representing jumps in the flux. The fluctuations are defined as

$$\mathcal{A}^-\Delta Q_{i-1/2} = \sum_{p:s_{i-1/2}^p<0} \mathcal{Z}_{i-1/2}^p \quad \text{and} \quad \mathcal{A}^+\Delta Q_{i-1/2} = \sum_{p:s_{i-1/2}^p>0} \mathcal{Z}_{i-1/2}^p \tag{7}$$

for the shallow water equations we are going to have

$$\begin{bmatrix} H_i - H_{i-1} \\ HU_i - HU_{i-1} \\ \varphi(Q_i) - \varphi(Q_{i-1}) \\ B_i - B_{i-1} \end{bmatrix} = \sum_{p=0}^{3} \alpha_{i-1/2}^p w_{i-1/2}^p \tag{8}$$

where $\varphi(q) = (hu^2 + \frac{1}{2}gh^2)$ is the momentum flux and B_i and B_{i-1} are cell-averaged approximations of the bathymetry of the respective cell.

In the GeoClaw solver adaptive mesh refinement (AMR) can be used. Multiple levels can be use where for each level the domain is specified. The topography for the problem is defined in a file. The topography goes into the shallow water equations through the right hand side B. The value from the file are converted into cell averages using a picewise bilinear function that interpolates the pointwise values. B is then obtained by evaluating the exact integral of this function over the cell.

4   The setup of the test case

The benchmark experiment was conducted in a 16.6 m long, 0.6m wide and 0.45 m deep wave tank. When a gate is lifted, it generates a single bore to impinge the column located downstream. We are going to simulate 2 cases in the experiment. The 1st case purely generated the single bore, the 2nd case generated the bore to impinge the column with one side facing the flow.

In the 1st case, wave height and streamwise velocity, U, at different depth, at where the center of column should be located are measured. In the 2nd case, the wave height in front and behind the column are measured.
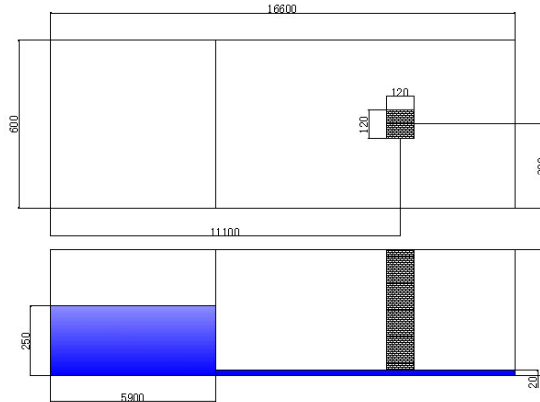

Figure 1: Diagram of experiment apparatus

In all cases below, boundary conditions are all set to reflection wall.

5 Dam Break

The initial condition for this and the following cases is given by

$$h_0(x, y) = \begin{cases} 0.25 & x < 5.9 \\ 0.02 & \text{otherwise} \end{cases} \tag{9}$$

$$u_0(x, y) = 0 \tag{10}$$

In this comparison we will include results from OpenFOAM, an open source CFD software modeling air and water using the Navier-Stokes equations with turbulence model. Figure 2 shows the time history of the wave height measured at the center location where the column will be mounted in the following cases. The result from GeoClaw agrees quite well in general(Show zoom in plot). At around t=3.8, GeoClaw accurately predicted the arrival of the shock. GeoClaw overestimates the peak water level a little, while OpenFOAM, gives a better value. After a later time, the wave gets reflected at the right wall of the tank, which can be seen by the second jump in wave height. GeoClaw also predicts the arrival time for this peak quite well but overestimates the peak value by a small amount.
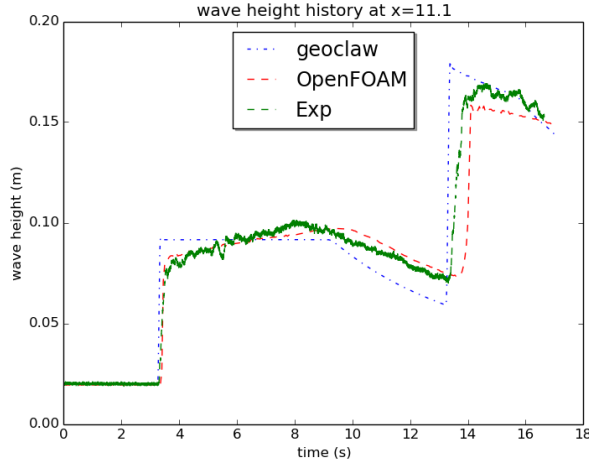

Figure 2: time history of wave height for case without a column.

Figure 3 shows the time history of the streamwise velocity u from GeoClaw and experiment. Note that this velocity u in both GeoClaw and experiment are depth-averaged. GeoClaw accurately predicted the time of the velocity peak as well as the value of the peak. After the initial jump in the velocity, GeoClaw overestimated the value of velocity. The reason why GeoClaw gives a higher velocity may be attributed to its depth-averaged property: Water at all depth are propagating with the same speed. In the experiment, the velocity is getting smaller the closer we get to the bottom.

6 Dam Break with square column

Figure 4 gives a comparison of the time history of the wave height measured at $0.04m$ ahead of the leading edge of the square column($0.1m$ ahead of center of the column). Note that this
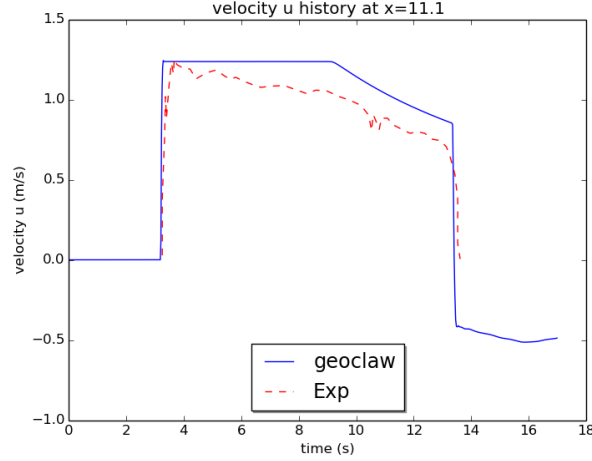
Figure 3: time history of streamwise velocity U for case without a column

figure is from $t = 3.0$ to $t = 4.0$, which shows a shorter range compared to the previous figures. There are two jumps in the result given by GeoClaw. A first jump with a change in water level from around 0.02 to 0.1 and a second jump from 0.1 to a higher level of around 0.22. If we recall from Figure 2 that the wave height is around 0.1, we can confirm that this first jump is caused by the shock wave originate in the dambreak. The second jump represents the wave reflected by the column. If we compare the time interval from the first to the second jump between measurement location $x = 11.0$ in Figure 4 and location 11.02 in Figure 7 we can see that as we get closer to the column, this time interval gets shorter.

There are two distinct differences between the GeoClaw and the experimental results. First, in the experiment, the dambreak causes a smooth increase in water height. Second, the arrival time of the peak predicted by GeoClaw is about 0.08 seconds ahead of the time measured in the experiment.

The difference in shock shape can be explained by the difference between the shallow water equations that GeoClaw solves and Navier-Stokes equations that better describe the physics. In shallow water equations, fluid viscosity is not taken into account, while it is significant in real physics. This causes the shock remain its shape as it propagates in shallow water equation while smooth out in experiment. Thus we see a jump in result from shallow water equation while a smooth increase in experiment result.

If we zoom in Figure 2 for smaller time range from $t = 3s$ to $t = 4s$, we get Figure 5. In Figure 5, arrival time of peak predicted by geoclaw is almost the same as that from experiment (only about 0.02 second earlier). This time interval is much smaller than that in Figure 4 though data are not measured at exactly the same point for this two plots. This difference indicates that the column gives more resistance to shock waves in experiment than it does in shallow water equation model.

A simple analysis to this phenomenon is draw as below. The shallow water equations are essentially a system of hyperbolic PDEs. The solution depends on initial condition along characteristics in the spatio-temporal domain. Thus before the propagating shock arrives, all water downstream the shock has zero velocity. In other words, it even does not know there

5

is a column before the shock hits the column. This can be verified by checking the history of the wave height measured at exactly the same location, $0.04m$ ahead of the leading edge of the square column, but in different cases, one with a square column and one without. This comparison is showed in Figure 6. As we expected, there is no difference in arrival time of the shock wave. In contrast, the Navier-Stokes equations are a system of PDEs of elliptic type. In real physics governed by Navier-Stokes equations, when front of the shock wave gets close to the column, water downstream it and upstream column are affected and resist the comming of wave to some extent. This slows down the propagating speed of shock wave when it comes close to the column in real world and thus shifts the peak toward later time in the plots.
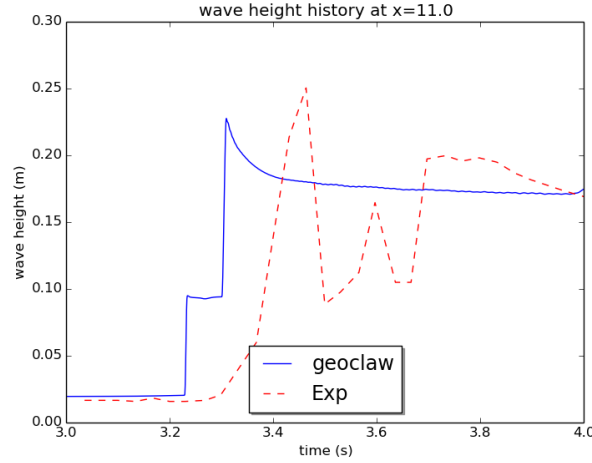

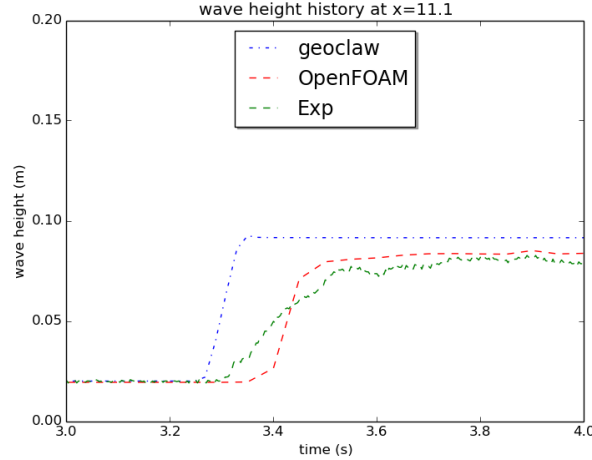Figure 4: time history of wave height for case with square column

Figure 5: time history of wave height for case without column (zoom in)

Figure 8 shows the time history of the wave height measured at the front face of the square column. The difference between the arrival time of the peak still exists as expected. After the peak arrives, the wave gradually becomes stable as indicated by a horizontal line in the plot. In this region the differences between GeoClaw and experiment are quite small.
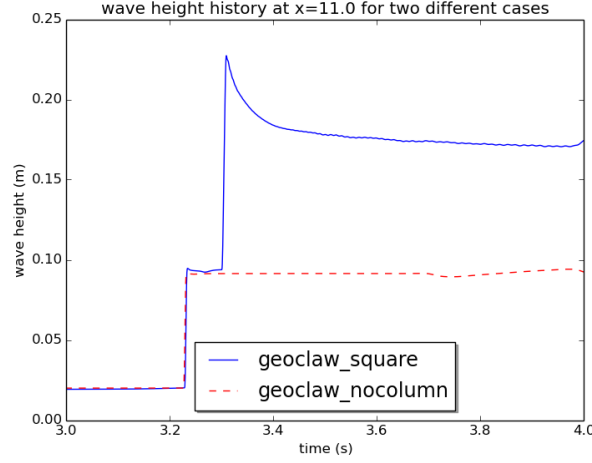
Figure 6: comparison of time history of wave height for case with a square column and case without one
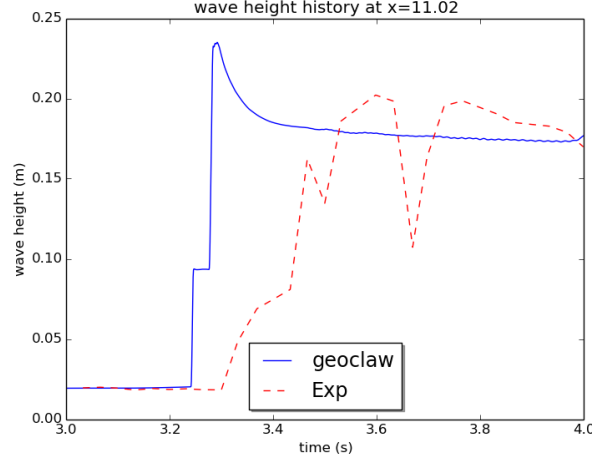

Figure 7: time history of wave height for case with square column, at x = 11.02

7   Dam Break with cylinder column

Figure 9 shows the time history of the wave height measured at $0.04m$ ahead of the leading edge of cylinder column($0.1m$ ahead of the center of the column). Similar feature as in the square column case Figure 4 can be found. However, the wave height at the second peak in this case is almost the same as that in square column case (around $0.22m$ in both case), while this feature is quite different for the experimental results between the two cases.

Note that diameter of the cylinder is equal to half the length of the square column. Thus the square column can block the flow in in a more efficient way than cylinder does, since the cylinder has a smoother shape for the fluid to pass by. This explains why we see a lower peak of wave height as well as less steep curve for history of wave height in case with the cylinder in the experiment. In GeoClaw, a geometry is represented with quadrilateral cells. In the
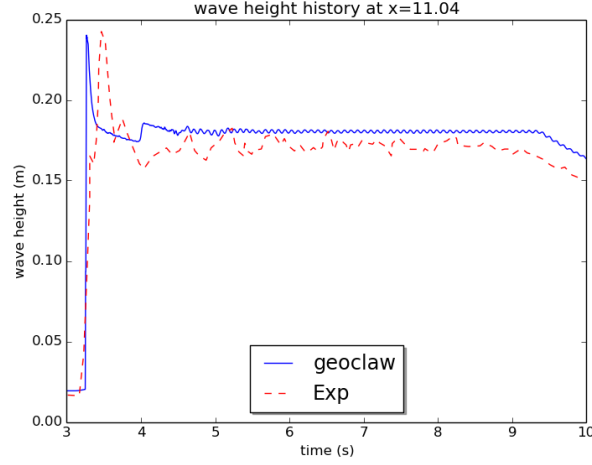
7

Figure 8: time history of wave height for case with square column, at x = 11.04

cylinder case, the cylinder is represented with square cells since our background mesh is simple structured quadrilateral mesh with square cells. Based on this, we can deduce in GeoClaw, when the shock wave hits the cylinder, it is hitting onto many small faces vertical to flow direction at different locations. Thus it is similar to hitting onto one big face vertical to flow direction, which is the case with square column. This is why my get similar result in GeoClaw for case with square column and case with cylinder.
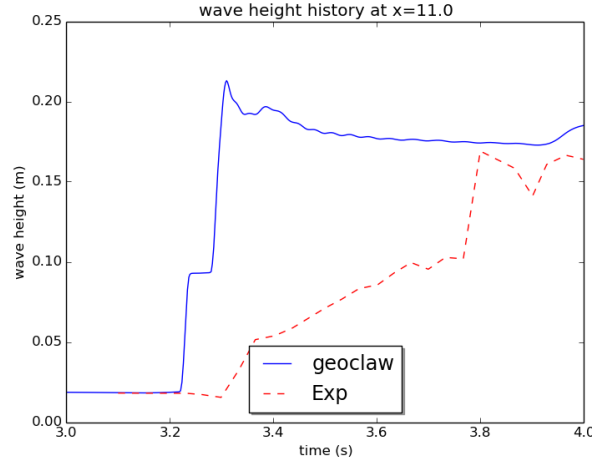

Figure 9: time history of wave height for case with cylinder column

Figure 10 shows the time history of the wave height for the cylinder case. As we expect, the peak predicted by GeoClaw appears earlier but the peak values agree quite well with the experiment. After the peak, GeoClaw gives a satisfied prediction of the wave height.
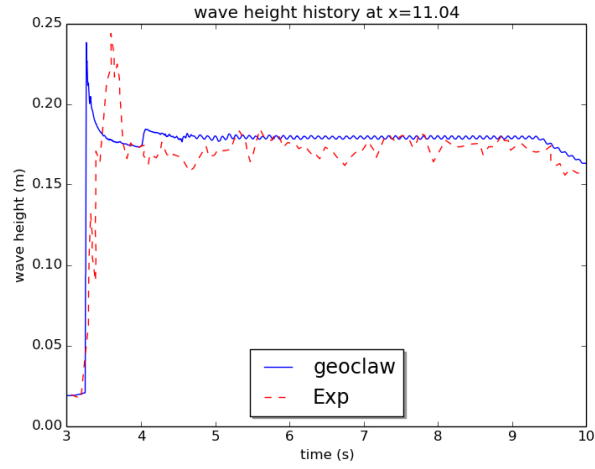
8

Figure 10: time history of wave height for case with cylinder column, at x = 11.04

8 Conclusion

References

[1] Halldór Árnason (2005). Thesis - Interactions between an incident bore and a free-standing coastal structure. http://faculty.washington.edu/cpetroff/Halldor%20dissertation.pdf

[2] David L. George (2008) Journal of Computational Physics - Augmented Riemann solvers for the shallow water equations over variable topography with steady states and inundation.

[3] Marsha J. Berger and David L. George and Randall J. LeVeque and Kyle T. Mandli (2011) Advances in Water Resources - The GeoClaw software for depth-averaged flows with adaptive refinement.